Iranian Journal of Basic Medical Sciences
ijbms.mums.ac.ir

Evaluation of excretory–secretory products of *Lucilia sericata* larvae loaded onto chitosan nanoparticles as a drug candidate against *Leishmania major*

Farzaneh Sadeghi [1], Mohammad Saaid Dayer [1]*, Fatemeh Ghaffarifar [2], Amrollah Azarm [1]

[1] Department of Medical Entomology, Faculty of Medical Sciences, Tarbiat Modares University, Tehran, Iran
[2] Department of Parasitology, Faculty of Medical Sciences, Tarbiat Modares University, Tehran, Iran

ARTICLE INFO

Article type:
Original

Article history:
Received: Apr 17, 2026
Accepted: Jul 22, 2026

Keywords:
Chitosan
Excretory-secretory products
Leishmaniasis
Leishmania major
Lucilia sericata

ABSTRACT

Objective(s): Zoonotic cutaneous leishmaniasis is an infectious disease caused by the protozoan parasite *Leishmania major* and characterized by chronic skin lesions. Treatment is often prolonged and associated with adverse effects. Chitosan, due to its favorable biomedical properties, including biocompatibility, biodegradability, non-toxicity, and wound-healing potential, has attracted considerable attention for therapeutic applications. This study aimed to evaluate the anti-leishmanial effects of excretory–secretory (ES) products of *Lucilia sericata* larvae loaded onto chitosan nanoparticles against *L. major* cells.

Materials and Methods: The ES was collected, filter-sterilized, and loaded onto chitosan nanoparticles (CN). The ES-loaded CN was applied at different concentrations under both *in vitro* and *in vivo* conditions to leishmanial cells, and its cytotoxicity was compared with that of the standalone CN, crude ES, and Glucantime as the first-line drug against cutaneous leishmaniasis caused by *L. major*.

Results: ES-loaded chitosan nanoparticles were more effective in healing leishmanial lesions than the crude ES and chitosan nanoparticles applied separately. The ES-loaded CN exhibited stronger inhibitory effects against both intracellular and extracellular forms of the parasite than its components did when used alone.

Conclusion: The results indicated that ES-loaded chitosan nanoparticles exerted antileishmanial and immunomodulatory effects on lesions. The formulation may therefore represent a promising alternative remedy for treating leishmanial lesions. Due to their biocompatibility, antimicrobial activity, and controlled-release capability, ES-loaded CN showed effective performance in wound healing and treatment.

▶ Please cite this article as:
Sadeghi F, Dayer MS, Ghaffarifar F, Azarm A. Evaluation of excretory–secretory products of *Lucilia sericata* larvae loaded onto chitosan nanoparticles as a drug candidate against *Leishmania major*. Iran J Basic Med Sci 2026; 29:

Introduction

Cutaneous leishmaniasis is considered one of the major public health challenges in tropical and subtropical regions, including Iran (1-3). The disease is caused by *Leishmania major* in rural areas and manifests as chronic cutaneous lesions often associated with psychosocial complications and permanent scarring (4, 5). Conventional treatments using pentavalent antimonial compounds, amphotericin B, and miltefosine face multiple limitations, including drug resistance, systemic toxicity, painful administration routes, and high treatment costs (6-9). These challenges highlight the urgent need to develop novel therapeutic strategies with improved efficacy and safety. In recent years, maggot therapy using *Lucilia sericata* larvae has been introduced as an effective biological treatment for chronic wounds (10-12). The therapeutic properties of these larvae are attributed to their excretory–secretory (ES) products, which contain various bioactive molecules such as lucifensin, antimicrobial peptides, proteolytic enzymes, and allantoin (13-15). These compounds exhibit antibacterial, debridement, and wound-healing properties (16, 17). However, the clinical application of ES products is limited by challenges related to stability and targeted delivery. Nanotechnology has provided innovative solutions for drug delivery through the development of advanced carrier systems (18, 19). Chitosan nanoparticles (CN), derived from the natural polysaccharide chitin, have gained significant attention due to their excellent biocompatibility, biodegradability, mucoadhesive properties, and intrinsic antimicrobial activity (20, 21). Their positive surface charge enables efficient encapsulation of bioactive compounds and facilitates controlled release and enhanced cellular uptake (22, 23). The combination of chitosan nanoparticles with therapeutic bioactive molecules represents a promising approach to improving treatment outcomes in infectious diseases (24, 25). Although previous studies have independently demonstrated the wound-healing potential of *L. sericata* ES products and chitosan nanoparticles, their combined application against parasitic infections has not been fully

***Corresponding author:** Mohammad Saaid Dayer. Jalal-e- Al-e-Ahmad Highway, Nasr, Tehran, Iran. Email: dayer@modares.ac.ir

investigated. Therefore, the present study aimed to evaluate the antileishmanial effects of ES products of *L. sericata* larvae loaded onto chitosan nanoparticles against *L. major* cells under both *in vitro* and *in vivo* conditions.

Materials and Methods

Rearing of Lucilia sericata and preparation of larval excretion/secretion (ES)

L. sericata flies were reared under insectarium conditions (temperature: 28 °C; relative humidity: 50±10%; photoperiodicity: 12:12 L/D) at Tarbiat Modares University. Fresh chicken liver was used to feed the larvae, while adult flies were provided with sugar water supplemented with a mixture of powdered milk and honey.

ES products were collected from second- and third-instar larvae of *L. sericata* under sterile conditions. Approximately 150 larvae were selected from a laboratory colony and starved for 6 hr to allow complete evacuation of the digestive tract. The larvae were then surface sterilized using 0.5% sodium hypochlorite for 2 min, followed by 1% formaldehyde for 2 min, and finally washed twice with sterile saline solution for 1 min. After sterilization, the larvae were transferred into sterile 50 ml Falcon tubes containing phosphate-buffered saline (PBS). The tubes were covered with aluminum foil to prevent evaporation and incubated at 37 °C for 2 hr to allow the release of larval excretory–secretory products. Following incubation, the ES-containing supernatant was carefully collected using sterile pipettes, transferred to sterile microtubes, and filtered through a sterile syringe filter to remove debris. The collected ES products were stored at −20 °C until further use.

Collection of larval excretion/secretion products

Larvae were first surface-sterilized using 0.5% sodium hypochlorite (2 min), 1% formaldehyde (2 min), and sterile saline (twice, 1 min each). To collect *L. sericata* excretion/secretion (ES) products, second- and third-instar larvae were starved for 12 hr and then incubated in phosphate-buffered saline (PBS) for 2 hr at 37 °C. ES products were aseptically collected from batches of 100 larvae and stored in 1.5 ml microtubes. The collected supernatant was passed through a syringe filter (13, 26, 27). Protein concentration of the crude ES extract was determined using the Bradford assay with bovine serum albumin (BSA) as the standard, and samples were stored at −20 °C until use (28, 29).

The total protein concentration of the ES products was determined using the Bradford protein assay. A standard curve was prepared using serial dilutions of bovine serum albumin (BSA) at concentrations ranging from 0 to 500 µg/ml. ES samples were mixed with Bradford reagent in microplate wells and incubated for 5 min at 25 °C in the dark to allow color development. Absorbance was measured at 595 nm using a microplate reader. All samples were analyzed in triplicate, and the mean absorbance values were used to quantify protein. The protein concentration of the samples was calculated using the linear regression equation obtained from the BSA standard curve and expressed in µg/ml.

Synthesis and characterization of chitosan nanoparticles

Chitosan nanoparticles were prepared according to the ionic gelation method. The chitosan (1% w/v) was dissolved in 1% acetic acid, and 0.5% sodium tripolyphosphate (TPP) was then added dropwise under magnetic stirring for 1 hr at room temperature. Nanoparticles were purified by centrifugation (12,000 rpm, 15 min) and washed three times with distilled water. To prepare ES-loaded chitosan nanoparticles, ES solution (2 mg/ml) was added during the gelation process (30, 31). Characterization was performed using dynamic light scattering (DLS) and Fourier-transform infrared (FTIR) spectroscopy (32).

Chitosan nanoparticles (CSNPs) were prepared using the ionic gelation method. Briefly, 1 g of high-molecular-weight chitosan was dissolved in 100 ml of distilled water under magnetic stirring. To facilitate dissolution, glacial acetic acid was added dropwise until the pH reached 4.5. Separately, a sodium tripolyphosphate (TPP) solution was prepared by dissolving 0.5 g of TPP in 100 ml of distilled water. To initiate nanoparticle formation, 50 ml of the TPP solution was added dropwise to 50 ml of the chitosan solution under vigorous magnetic stirring at room temperature. The mixture was stirred for 1 hr to ensure complete cross-linking. The resulting nanoparticle suspension was centrifuged at 12,000 ×g for 15 min, and the supernatant containing unreacted compounds was discarded. The pellet was washed three times with sterile distilled water, followed by centrifugation, to obtain purified plain CSNPs.

Preparation of ES-loaded chitosan nanoparticles (ES-CSNPs)

To prepare ES product-loaded chitosan nanoparticles (ES-CSNPs), 50 ml of the crude ES solution (2 mg/ml) was gently mixed with 50 ml of the chitosan solution under magnetic stirring. Subsequently, 50 ml of the TPP solution (0.5% w/v) was added dropwise to the mixture while stirring. The suspension was stirred for 1 hr until the encapsulation process was completed. The ES-CSNPs were collected by centrifugation at 12,000 ×g for 15 min, washed three times with sterile distilled water, and stored at 4 °C for further characterization and biological assays. All preparation steps were carried out under sterile conditions.

Physicochemical characterization

The physicochemical characteristics of the synthesized nanoparticles were determined using DLS and FTIR. Before analysis, the nanoparticle suspensions were subjected to ultrasonication for 30 min to ensure uniform dispersion. DLS analysis (Malvern Zetasizer) revealed that the plain CSNPs had a mean size of 150–200 nm, a polydispersity index (PDI) of<0.3, and a positive zeta potential of +30 to +35 mV, indicating good colloidal stability.

Parasite culture

L. major promastigotes were cultured in RPMI-1640 supplemented with 10% fetal bovine serum (FBS) and penicillin–streptomycin (100 µg/ml) at 26 °C. The murine macrophage cell line J774A.1 was maintained in DMEM with 10% FBS at 37 °C in 5% CO_2. Both cultures were monitored regularly and passaged in the logarithmic phase of growth (33, 34).

In vitro assays

Promastigotes (1×10^6 cells/ml) were treated with serial concentrations (0-500 µg/ml) of chitosan nanoparticles, ES-loaded nanoparticles, crude ES material, and Glucantime (positive control) in 96-well plates. Viability was assessed at 24, 48, and 72 hr using Neubauer slide counting (35, 36).

MTT cytotoxicity assay

Macrophages (1×10^5 cells/well) were treated with different concentrations of the test compounds for 72 hr. MTT solution (5 mg/ml) was added, and the macrophages were then incubated for 4 hr. Formazan crystals were dissolved, and absorbance was measured at 570 nm. The

percentage of cell viability was calculated, and DMSO IC_{50} and CC_{50} values were determined from the dose-response curves. The selectivity index (SI) was calculated as the ratio CC_{50}/IC_{50} (37, 38).

In vivo study

Animal model: Twenty-five mice (BALB/c) were infected subcutaneously at the base of the tail with stationary-phase promastigotes (1×10^6). Lesion formation was monitored weekly until ulceration (approximately 5 weeks post-infection). The experimental groups were then divided as follows:

- Group 1: Glucantime (20 mg/kg, intraperitoneal)
- Group 2: Raw ES (350 µg/ml, topical)
- Group 3: Chitosan nanoparticles (50 mg/kg, topical)
- Group 4: ES-loaded chitosan nanoparticles (50 mg/kg containing 350 µg/ml ES, topical).
- Group 5: Negative control (no treatment)

Lesion size was measured weekly with digital calipers. At week 8 post-treatment, the mice were anesthetized, and spleen samples were collected. Parasite burden was determined by limiting dilution assay. Spleen homogenates were serially diluted in complete medium and monitored for promastigote growth for 10-14 days. Parasite burden was calculated as the negative logarithm of the number of parasites per gram of tissue (39, 40).

A total of 25 female BALB/c mice (4 weeks old) were obtained from the Royan Institute and used in the *in vivo* experiments. The animals were randomly assigned to five experimental groups (n=5 per group) and housed in separate cages under standard laboratory conditions (temperature 22±2 °C, humidity 55±5%, and a 12 h light/dark cycle). Food and water were provided *ad libitum*. All experimental procedures were conducted in accordance with institutional guidelines for the care and use of laboratory animals and approved by the Animal Ethics Committee of Tarbiat Modares University (Ethical code: IR.MODARES.AEC.1403.051).

The progression of cutaneous lesions was monitored weekly throughout the experimental period. Lesion dimensions (length, width, and height) were measured using digital calipers, and the recorded measurements were used to evaluate the therapeutic response in different treatment groups. These measurements were performed systematically during the monitoring period to assess lesion progression and healing.

Statistical analysis

All experiments were performed in triplicate. Data were analyzed using one-way ANOVA and Mann-Whitney tests in SPSS software (version 26). Results are presented as mean±standard deviation, and $P<0.05$ was considered the level of significance (41, 42).

All experiments were performed in three independent replicates. Statistical analyses were conducted using SPSS software (version 26) and Microsoft Excel. Data were expressed as mean±standard deviation (Mean±SD). Differences among multiple groups were analyzed using one-way analysis of variance (ANOVA), while pairwise comparisons were performed using the Mann–Whitney U test when appropriate. A *P*-value of less than 0.05 ($P<0.05$) was considered statistically significant.

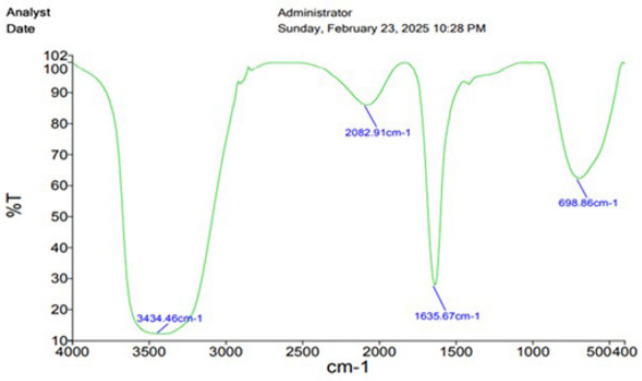

Figure 1. Fourier-transform infrared (FTIR) spectrum for characterization of chitosan nanoparticles

Results

Preparation of Larval ES products and protein concentration assay

The protein concentration of the crude ES extract was determined using a standard curve generated with BSA (50-100 mg). The results showed that the mean net absorbance of the crude ES sample at 595 nm was 1.961, corresponding to a mean protein concentration of 824 µg/ml.

Synthesis and characterization of chitosan nanoparticles (CSNPs)

Chitosan nanoparticles were successfully synthesized via the ionic gelation method to serve as carriers for the ES extract and were also tested independently. FTIR spectroscopy was used to confirm the chemical structure of the chitosan nanoparticles. The obtained spectrum showed characteristic peaks at 3434 cm^{-1} (stretching vibrations of O-H and N-H, indicating hydroxyl and amine groups), 1635 cm^{-1} (C=O stretching vibration related to amide I, confirming the presence of chitosan amide groups), and 698 cm^{-1} (C-H bending of the glycosidic ring). A minor peak at 2082 cm^{-1} was considered insignificant and likely related to overtone vibrations (Figure 1).

DLS was used to determine the hydrodynamic size distribution of the nanoparticles. The main peak was observed at 485 nm, confirming the nanometric size of the primary particles, although some aggregation was observed (Figure 2).

In vitro anti-leishmanial activity

The inhibitory effects of crude ES, free-standing chitosan nanoparticles (CSNPs), and ES-loaded chitosan nanoparticles (ES-CSNPs) on the viability of *L. major* promastigotes over 72 hr were evaluated. The half-maximal inhibitory concentration (IC_{50}) for each treatment was calculated.

The IC_{50} value for crude ES was approximately 1050 µg/ml, which was similar to the positive control (Glucantime, ~1000 µg/ml), indicating no significant difference in inhibitory effect. For free-standing CSNPs, a reliable IC_{50} value could not be obtained due to a non-sigmoidal dose-response curve, suggesting low intrinsic anti-leishmanial activity of these nanoparticles.

In contrast, the ES-CSNPs formulation showed significantly higher inhibitory potency, with an IC_{50} of approximately 500 µg/ml at 72 hr. This IC_{50} was significantly lower than that of the positive control ($P<0.0001$), indicating superior inhibitory activity. Microscopic observations revealed that promastigotes treated with ES-CSNPs initially lost motility, became spherical,

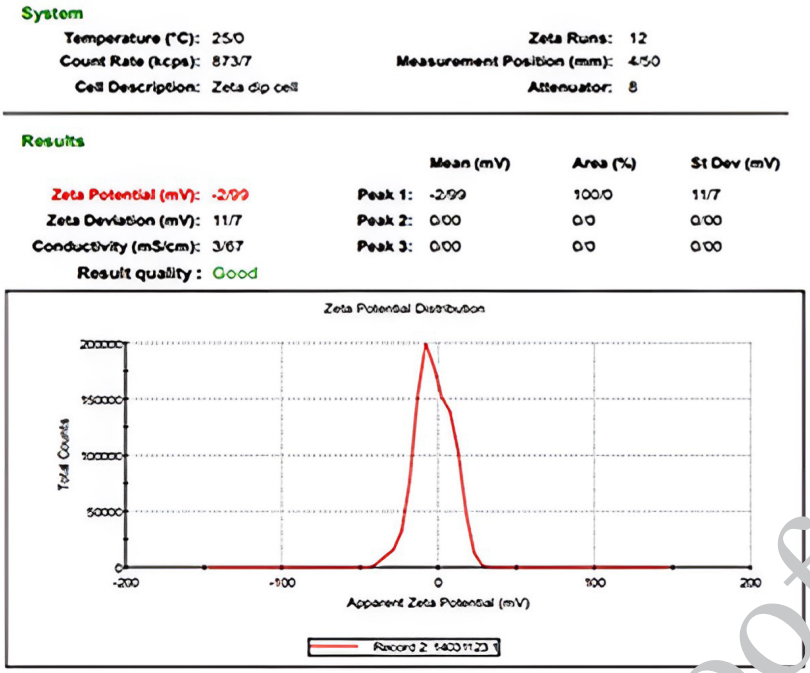

Figure 2. Outcome of dynamic light scattering (DLS) for determining the hydrodynamic size distribution of nanoparticles peaking at 485 nm

and eventually disintegrated and disappeared. The lethal effect was dose- and time-dependent.

Cellular toxicity evaluation (MTT assay)

The potential toxicity of the treatments on murine macrophage J774A.1 cells was assessed after 72 hr of exposure using the MTT assay. Results showed that ES-loaded nanoparticles (ES-CSNPs) significantly affected macrophage viability ($P<0.05$) in a dose-dependent manner. However, no statistically significant cellular toxicity was observed for crude ES ($P=0.9706$), plain CSNPs ($P=0.3464$), or Glucantime compared to the untreated control. These results indicate that the ES-CSNPs formulation, despite its high efficacy against the parasite, has a selective toxicity profile, meaning it is more toxic to the parasite than to host macrophages at the tested concentrations.

In vivo therapeutic efficacy in BALB/c mice

The therapeutic potential of the formulations was evaluated in a murine model of cutaneous leishmaniasis caused by *L. major*. Skin lesions began to appear in infected BALB/c mice starting in the fourth week post-infection. Lesion size was measured weekly. In the negative control group, the mean lesion size progressively increased to 9.97±1.98 mm² by the fifth week. In contrast, all treatment groups showed a gradual decrease in lesion size during therapy.

A statistically significant difference ($P<0.0001$) in lesion size reduction was observed between the ES-CSNPs-treated group and the Glucantime-treated group, indicating the better efficacy of the nanoparticle formulation. The differences between the crude ES and plain CSNPs groups compared with Glucantime were not significant. Furthermore, during the 12-week study period, no mortality was observed in the ES-CSNPs-treated group, highlighting the safety of this formulation in the animal model (Figure 3).

Parasite burden in the spleen

Ten days after the end of the treatment period, the parasite

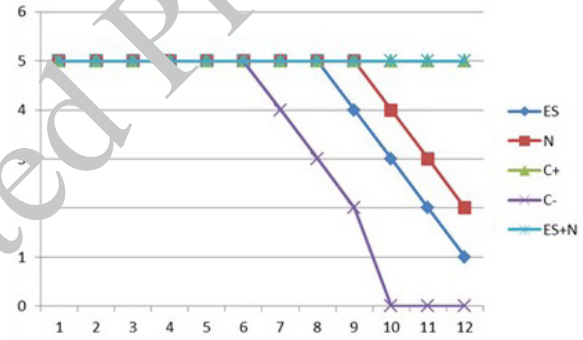

Figure 3. Survival outcomes of mice following 4 weeks of treatment and 8 weeks post-treatment
C+: Glucantime-treated positive control; C−: Untreated negative control; ES+N: Lucilia sericata excretory-secretory products loaded on chitosan nanoparticles

burden in the spleens of infected mice was measured using the limiting dilution method. A significant reduction in parasite burden was observed in all treated groups compared to the negative control. The parasite burden was significantly lower in the ES-CSNPs-treated group than in the Glucantime group, indicating a higher ability of this formulation to control the progression of systemic infection. No significant difference was found between the crude ES- and CSNP-treated groups in splenic parasite burden (Figure 4).

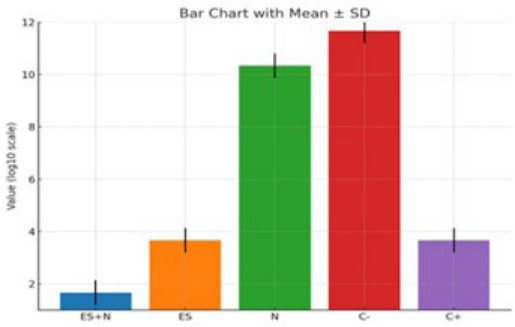

Figure 4. Parasite burden test results in the four mouse study groups

Table 1. Mean lesion diameter (mm±standard deviation) in different mouse experimental groups over time (Weeks 1-4: Treatment period. Weeks 5-8: follow-up period)

Week	PC	NC	Cr ES	CN	ES+ CN
1	6.44±2.72	7.58±2.14	6.58±2.63	6.56±2.82	6.40±2.65
2	5.94±1.65	7.87±2.16	5.89±2.12	5.87±1.98	5.35±1.43
3	4.15±1.34	8.80±1.68	4.20±1.87	5.20±1.87	4.13±1.26
4	3.82±1.65	9.23±2.16	3.90±1.76	3.90±1.76	3.67±1.19
5	2.92±1.34	9.97±1.98	3.10±1.56	3.20±1.67	2.82±1.23
6	1.95±1.65	10.28±1.68	2.10±1.56	2.20±1.58	1.87±1.18
7	1.43±1.20	11.47±1.98	1.68±1.56	1.89±1.67	1.29±1.40
8	1.53±1.40	12.56±2.16	1.77±1.48	1.83±1.54	1.10±1.10*

Note: P.C.: Positive Control (Glucantime). N.C.: Negative Control, Cr. ES: Crude Larval Extract, C.N.: Chitosan Nanoparticles, ES+C.N.: ES-loaded Chitosan Nanoparticles

Mean diameters of progressive lesions

The progression and healing of lesions were carefully tracked by measuring the mean lesion diameter over eight weeks (Table 1). The results showed a clear therapeutic trend. Although all treatment groups showed improvement, Group 5 (treated with ES-CSNPs) consistently had the smallest lesion diameter from the third week onward. By week eight, the mean lesion diameter in this group was 1.10±1.1 mm; in the positive control (Glucantime), it was 1.53±1.4 mm, and in the negative control, it was 12.56±2.16 mm. Statistical analysis (ANOVA) confirmed that the mean lesion size in Group 5 was significantly smaller than in the other groups (P<0.05), wound progression was effectively halted, and fresh tissue growth was observed at the lesion site.

Discussion

The present study was conducted to investigate the anti-leishmanial effects of (ES) materials against *L. major* cells under *in vitro* and *in vivo* conditions. This study demonstrated that loading the larval ES materials of *L. sericata* on chitosan nanoparticles significantly enhanced the anti-leishmanial activity of *L. sericata* ES under both *in vitro* and *in vivo* conditions. This increase in efficacy is likely attributable to a synergistic effect between the antimicrobial peptide compounds present in the larval extract and the permeability properties and controlled-release capability of chitosan nanoparticles. The findings of this research regarding the strong inhibitory effects of larval products on leishmanial promastigotes are consistent with the results of previous studies and suggest their potential as candidates for the treatment of cutaneous leishmaniasis (43, 44).

One important aspect of the development of new drugs is their selective toxicity, meaning the drug should be lethal to the parasite while remaining safe for host cells. In this study, the larval ES of *L. sericata* exhibited strong toxicity on J774A.1 macrophage cell line. This finding aligns with previous reports by other researchers. The results of this study indicated that the ES-CSNP formulation (ES-loaded chitosan nanoparticles) was significantly more effective than the crude ES or plain nanoparticles. Lower IC_{50} values under *in vitro* conditions, improved healing of skin lesions, and a lower parasite burden in *in vivo* models indicated the higher effectiveness of the ES-CSNP formulation. Chitosan nanoparticles likely enhance this efficacy through multiple mechanisms. According to previous studies, chitosan nanoparticles have been shown to improve drug delivery remarkably (45).

The *in vivo* results of this study showed significant improvement in skin lesions in BALB/c mice treated with ES-CSNP, which is consistent with, and superior to, the findings of studies that used live larvae or crude ES. Although precise identification of the mechanism of action requires further investigation, observations from this research and prior studies suggest several possible mechanisms. The antimicrobial peptide compounds (AMPs) present in ES, such as lucifensin, may cause parasite death by disrupting the parasite's cell membrane. These compounds may also act by inducing programmed cell death (apoptosis) in the parasite, leading to its demise. Furthermore, ES components may interfere with vital metabolic or signaling pathways, thereby killing the parasite (45-47).

Conclusion

In the present study, a single therapeutic dose was selected for each treatment formulation based on previously reported studies and experimental feasibility. Therefore, a comprehensive dose–response evaluation was not performed. Future studies are required to investigate the dose-dependent therapeutic efficacy of ES-loaded chitosan nanoparticles in experimental models of cutaneous leishmaniasis.

Although the present study demonstrates the therapeutic potential of ES-loaded chitosan nanoparticles against experimental cutaneous leishmanial cells, the efficacy of this formulation against drug-resistant strains of *L. major* was not directly evaluated. Therefore, further investigations are necessary to determine whether this formulation could be effective in drug-resistant cases.

Acknowledgment

The authors would like to acknowledge the financial support of Tarbiat Modares University, Iran. They also wish to thank members of the Department of Medical Entomology for their assistance. The results described in this paper were part of the student's thesis.

Ethical Considerations

This study was approved by the Ethics Committee of Tarbiat Modares University (Approval No. IR.MODARES.AEC.1403.051).

Authors' Contributions

F S contributed to conceptualization, investigation, data curation, visualization, and writing the original draft. MS D handled conceptualization, methodology, supervision, software development, and final review and editing. F G was responsible for visualization, investigation, and final writing, review, and editing. A A contributed through investigation, software, methodology, validation, and final review and editing.

Conflicts of Interest

The authors declare there are no conflicts of interest.

Declaration

An artificial intelligence (Chatgpt) tool was used solely for final English language editing and improving the clarity and readability of the manuscript.

References

1. Firooz A, Mortazavi H, Khamesipour A, Ghiasi M, Abedini R, Balighi K, *et al*. Old world cutaneous leishmaniasis in Iran: Clinical variants and treatments. J Dermatolog Treat 2021;32:673-683.
2. Holakouie-Naieni K, Mostafavi E, Boloorani AD, Mohebali M, Pakzad R. Spatial modelling of cutaneous leishmaniasis in Iran from 1983 to 2013. Acta Tropica 2017;166:67-73.
3. Mahmoudzadeh-Niknam H, Ajdary S, Riazi-Rad F, Mirzadegan E, Rezaeian A, Khaze V, *et al*. Molecular epidemiology of cutaneous leishmaniasis and heterogeneity of *Leishmania major* strains in Iran. Trop Med Int Health 2012;17:1335-1344.
4. Jafari R, Abdoli H, Arandian MH, Shareghi N, Ghanei M, Jalali-Zand N, *et al*. Emerging of cutaneous leishmaniasis due to *Leishmania major* in a new focus in Esfahan Province, Central Iran. J Arthropod Borne Dis 2020;14:134.
5. Norouzinezhad F, Ghaffari F, Norouzinejad A, Kaveh F, Gouya MM. Cutaneous leishmaniasis in Iran: Results from an epidemiological study in urban and rural provinces. Asian Pac J Trop Biomed 2016;6:614-619.
6. Khamesipour A, Mohammadi A, Jaafari M, Fakandeh S, Tasbihi M, Javadi A, *et al*. Pilot study of safety and efficacy of topical liposomal amphotericin B for cutaneous leishmaniasis caused by *Leishmania major* in the Islamic Republic of Iran. East Mediterr Health J 2022;28:658-663.
7. Reithinger R, Dujardin J-C, Louzir H, Pirmez C, Alexander B, Brooker S. Cutaneous leishmaniasis. Lancet Infect Dis 2007;7:581-596.
8. Minodier P, Parola P. Cutaneous leishmaniasis treatment. Travel Med Infect Dis 2007;5:150-158.
9. Singh S, Sivakumar R. Challenges and discoveries in the treatment of leishmaniasis. J Infect Chemother 2004;10:307-315.
10. Gazi U, Taylan-Ozkan A, Mumcuoglu KY. The effect of *Lucilia sericata* larval excretion/secretion (ES) products on cellular responses in wound healing. Med Vet Entomol 2021;35:257-266.
11. Bexfield A, Bond A, Morgan C, Wagstaff J, Newton R, Ratcliffe N, *et al*. Amino acid derivatives from *Lucilia sericata* excretions/secretions may contribute to the beneficial effects of maggot therapy via increased angiogenesis. Br J Dermatol 2010;162:554-562.
12. Nigam Y, Dudley E, Bexfield A, Bond AE, Evans J, James J. The physiology of wound healing by the medicinal maggot, *Lucilia sericata*. Adv Insect Physiol 2010;39:39-81.
13. Tombulturk FK, Kanigur-Sultuybek G. A molecular approach to maggot debridement therapy with *Lucilia sericata* and its excretions/secretions in wound healing. Wound Repair Regen 2021;29:1051-1061.
14. Nezakati E, Hasani MH, Zolfaghari P, Rashidan M, Sohrabi MB. Effects of *Lucilia sericata* maggot therapy in chronic wound treatment: A randomised clinical trial. Chronic Wound Care Manag Res 2020:11-17.
15. Wang D, Tang X, Ruan J, Zhu Z, Wang R, Weng Y, *et al*. HSP90AB1 as the druggable target of maggot extract, reverses cisplatin resistance in ovarian cancer. Oxid Med Cell Longev 2023;2023:9335440.
16. Alipour H, Shahriari-Namadi M, Ebrahimi S, Moemenbellah-Fard MD. Wound healing potential: Evaluation of molecular profiling and amplification of *Lucilia sericata* angiopoietin-1 mRNA mid-part. BMC Res Notes 2020;13:308.
17. Valachova I, Bohova J, Kozanek M, Takac P, Majtan J. *Lucilia sericata* medicinal maggots: A new source of antimicrobial compounds. Microbial Pathogens and Strategies for Combating Them: Science, Technology and Education. Badajoz, Spain: Formatex Research Center. 2013:1745-1753.
18. Sim S, Wong NK. Nanotechnology and its use in imaging and drug delivery. Biomed Rep 2021;14:42.
19. Park K. Nanotechnology: What it can do for drug delivery. J Control Release 2008;120:1.
20. Saeedi M, Vahidi O, Moghbeli MR, Ahmadi S, Asadnia M, Akhavan O, *et al*. Customizing nano-chitosan for sustainable drug delivery. J Control Release 2022;350:175-192.
21. Divya K, Jisha M. Chitosan nanoparticles preparation and applications. Environ Chem Lett 2018;16:101-112.
22. Aibani N, Rai R, Patel P, Cuddihy G, Wasan EK. Chitosan nanoparticles at the biological interface: Implications for drug delivery. Pharmaceutics 2021;13:1686.
23. Nagpal K, Singh SK, Mishra DN. Chitosan nanoparticles: A promising system in novel drug delivery. Chem Pharm Bull (Tokyo) 2010;58:1423-1430.
24. Landriscina A, Rosen J, Friedman AJ. Biodegradable chitosan nanoparticles in drug delivery for infectious disease. Nanomedicine 2015;10:1609-1619.
25. Divakar DD, Jastaniyah NT, Altamimi HG, Alnakhli YO, Al Kheraif AA, Haleem S. Enhanced antimicrobial activity of naturally derived bioactive molecule chitosan conjugated silver nanoparticle against dental implant pathogens. Int J Biol Macromol 2018;108:790-797.
26. Sherafati J, Dayer MS, Ghaffarifar F, Akbarzadeh K, Pirestani M. Evaluating leishmanicidal effects of *Lucilia sericata* products in combination with *Apis mellifera* honey using an *in vitro* model. PLoS One 2023;18:e0283355.
27. Sherafati J, Dayer MS, Ghaffarifar F. Therapeutic effects of *Lucilia sericata* larval excretion/secretion products on *Leishmania major* under *in vitro* and *in vivo* conditions. Parasit Vectors 2022;15:212.
28. Firoozfar F, Moosa-Kazemi SH, Rafinejad J, Saghafipour A, Baniardalani M, Ahmed Yusuf M, *et al*. Environmental factors influencing the growth of *Lucilia Sericata* larvae used for maggot therapy under laboratory condition. J Kerman Univ Med Sci 2018;25:118-127.
29. Bagheri M, Alipour H, Shahriari-Namadi M, Malekpour SH, Raz A. Improving maggot therapy: Mass rearing and molecular identification of *Lucilia Sericata* (Meigen, 1826) Larvae In Maggotarium, School of Health, Shiraz. 2021.
30. Nguyen TA, Nguyen TH. Study on fabrication of antibacterial low molecular weight nanochitosan using sodium tripolyphosphate and hydrogen peroxide. J Nanotechnol 2022;2022:8368431.
31. Simin A, Ghaffarifar F, Delavari H, Dayer MS, Hamidianfar N, Baghkhani F. *In vitro* and *in vivo* effects of ethanolic extract of *Fumaria parviflora* Lam. embedded in chitosan nanoparticles against *Leishmania major*. Acta Parasitol 2024;69:628-638.
32. Van Bavel N, Issler T, Pang L, Anikovskiy M, Prenner EJ. A simple method for synthesis of chitosan nanoparticles with ionic gelation and homogenization. Molecules 2023;28:4328.
33. Soltani S, Mojiri-Forushani H, Soltani S, Kahvaz MS, Foroutan M. Evaluation of antileishmanial activity employing conventional and solid lipid nanoparticles of amphotericin B on *Leishmania major in vitro* and *in vivo*. Infect Disord Drug Targets 2020;20:822-827.
34. Maleki F, Zarebavani M, Mohebali M, Dayer MS, Hajialiani F, Tabatabaie F. *In vitro* and *in vivo* susceptibility of *Leishmania major* to some medicinal plants. Asian Pac J Trop Biomed 2017;7:37-42.

35. Azizi K, Shahidi-Hakak F, Asgari Q, Hatam GR, Fakoorziba MR, Miri R, Moemenbellah-Fard MD. *In vitro* efficacy of ethanolic extract of *Artemisia absinthium* (Asteraceae) against *Leishmania major* L. using cell sensitivity and flow cytometry assays. J Parasit Dis 2016;40:735-740.
36. Zarandi HZ-A, Shirani-Bidabadi L, Aghaei-Afshar A, Eghbalian M, Zolala J, Mirtadzadini M, *et al*. *In vitro* evaluation of hydroalcoholic extracts of *Capparis spinosa*, *Ricinus communis*, and *Solanum luteum* on *Leishmania major* (MRHO/IR/75/ER) Promastigotes. Jundishapur J Nat Pharm Prod 2021;17:e115306.
37. Basmaciyan L, Azas N, Casanova M. Different apoptosis pathways in *Leishmania parasites* cell death discovery. 2018;4:90.
38. Khamesipour F, Khamesipour A, Hejazi SH, Ghanadian M. *In vitro* assessment of *Dracocephalum lindbergii* for growth inhibition, apoptosis induction, and cytokine modulation against *Leishmania major*. Heliyon 2024;10:e38331.
39. Feiz Haddad MH, Rezvan H, Ghasemi M, Mohseni E, Dalvand R, Hamoonnavard S, Habibpour H. Cellular and histopathological changes in BALB/c mice infected with live attenuated *Leishmania major* parasite. Archives of Razi Institute. 2026; 81:353-364.
40. Carrion J, Nieto A, Iborra S, Iniesta V, Soto M, Folgueira C, *et al*. Immunohistological features of visceral leishmaniasis in BALB/c mice. Parasite Immunol 2006;28:173-183.
41. Zahirnia AH, Bordbar A, Ebrahimi S, Spotin A, Mohammadi S, Ghafari SM, *et al*. Predominance of *Leishmania major* and rare occurrence of *Leishmania tropica* with haplotype variability at the center of Iran. Braz J Infect Dis 2018;22:278-287.
42. Lopes ME, Dos Santos LM, Sacks D, Vieira LQ, Carneiro MB. Resistance against *Leishmania major* infection depends on microbiota-guided macrophage activation. Front Immunol 2021;12:730437.
43. Rahimi S, Khamesipour A, Akhavan AA, Rafinejad J, Ahmadkhaniha R, Bakhtiyari M, *et al*. The leishmanicidal effect of *Lucilia sericata* larval saliva and hemolymph on *in vitro Leishmania tropica*. Parasit Vectors 2021;14:40.
44. Sanei-Dehkordi A, Khamesipour A, Akbarzadeh K, Akhavan AA, Mohammadi AMA, Mohammadi Y, *et al*. Anti Leishmania activity of *Lucilia sericata* and *Calliphora vicina* maggots in laboratory models. Exp Parasitol2016;170:59-65.
45. Akküçük Ş, Kaya ÖM, Yaman M. What is the best animal model for leishmaniasis studies? Turkish J Vet Res 2018;2:28-31.
46. Song M, Bai X, Wang D, Wang Q, Pan L, He P, *et al*. Combined application of moist exposed burn ointment and maggot therapy in wound healing. J Wound Care2022;31:S41-S52.
47. Benbow M. Modern wound therapies: Maureen Benbow gives an overview of just some of the vast range of modern wound therapies available to community nurses. J Community Nurs 2008;22:20-25.